Supplementary Information for

Amplified warming from physiological responses to carbon dioxide reduces the potential of vegetation for climate change mitigation

Mingzhu He[1], Shilong Piao[1,2*], Chris Huntingford[3], Hao Xu[1], Xuhui Wang[1], Ana Bastos[4], Jiangpeng Cui[1], Thomas Gasser[5]

[1]Sino-French Institute for Earth System Science, College of Urban and Environmental Sciences, Peking University, Beijing 100871, China.

[2]Institute of Tibetan Plateau Research, Chinese Academy of Sciences, Beijing 100101, China.

[3]UK Centre for Ecology and Hydrology, Wallingford, Oxfordshire OX10 8BB, UK.

[4]Department of Biogeochemical Integration, Max Planck Institute for Biogeochemistry, Jena 07745, Germany

[5]International Institute for Applied Systems Analysis, Laxenburg A-2361, Austria.

*Corresponding author: Shilong Piao (slpiao@pku.edu.cn)

Supplementary Table 1 Descriptions of different effects of increasing atmospheric CO_2. Calculations of ALL, RAD, PHY_{all}, PHY_{dir} and PHY_{int} effects from increasing atmospheric CO_2 using 1pctCO2, esmFdbk1 and esmFixClim1 simulations. 1pctCO2 scenario indicates that both atmosphere and land surface experience 1% per year cumulative increase in CO_2, while esmFedbk1 scenario indicates that only effects of increasing CO_2 concentration on atmosphere, and esmFixClim1 scenario indicated that only land surface is affected by increasing CO_2 concentration.

Name	Calculations per year	Calculations at 4 × CO_2
ALL	Each year in 1pctCO2 minus average of year 1-20 in 1pctCO2	Average of year 121-140 in 1pctCO2 minus average of year 1-20 in 1pctCO2
RAD	Each year in esmFdbk1 minus average of year 1-20 in esmFdbk1	Average of year 121-140 in esmFdbk1 minus average of year 1-20 in esmFdbk1
PHY_{all}	Each year in 1pctCO2 minus each year in esmFdbk1	Average of year 121-140 in 1pctCO2 minus average of year 121-140 in esmFdbk1
PHY_{dir}	Each year in esmFixClim1 minus average of year 1-20 in esmFixClim1	Average of year 121-140 in esmFixClim1 minus average of year 1-20 in esmFixClim1
PHY_{int}	PHY_{all} minus PHY_{dir}	PHY_{all} minus PHY_{dir}

Supplementary Table 2 Area-weighted values for different variables at 4 × CO_2 across global vegetated land. PHY_{all} is calculated as the difference between average of the last 20 years from 1pctCO2 and average of the last 20 years from esmFdbk1, and PHY_{dir} is calculated as the difference between average of the last 20 years in esmFixClim1 and average of the first 20 years from the same scenario (esmFixClim1).

	PHY_{all}	PHY_{dir}
Leaf area index (LAI; m^2 m^{-2})	0.69	0.56
Cloud fraction (%)	-1.02	-0.91
Net Longwave radiation (W m^{-2})	-1.25	-1.56
Albedo	-0.0032	-0.0041
Aerodynamic resistance (r_a; s m^{-1})	-8.74	-6.87
Evapotranspiration (ET; mm d^{-1})	-0.09	-0.11
Downwelling shortwave radiation (SW; W m^{-2})	2.14	1.80
Air emissivity (ε_a)	-0.0022	-0.0029

Supplementary Figure 1 Changes in global carbon storage induced by the total CO_2 physiological (PHY_{all}), radiative (RAD) and the coupled (ALL) forcings in response to increasing atmospheric CO_2. The solid lines correspond to the multi-model mean, while the shaded area indicates the standard error across five ESMs, including CanESM2, CESM1-BGC, HadGEM2-ES, IPSL-CM5A-LR and MPI-ESM-LR, as bcc-csm1-1 does not have carbon storage outputs.

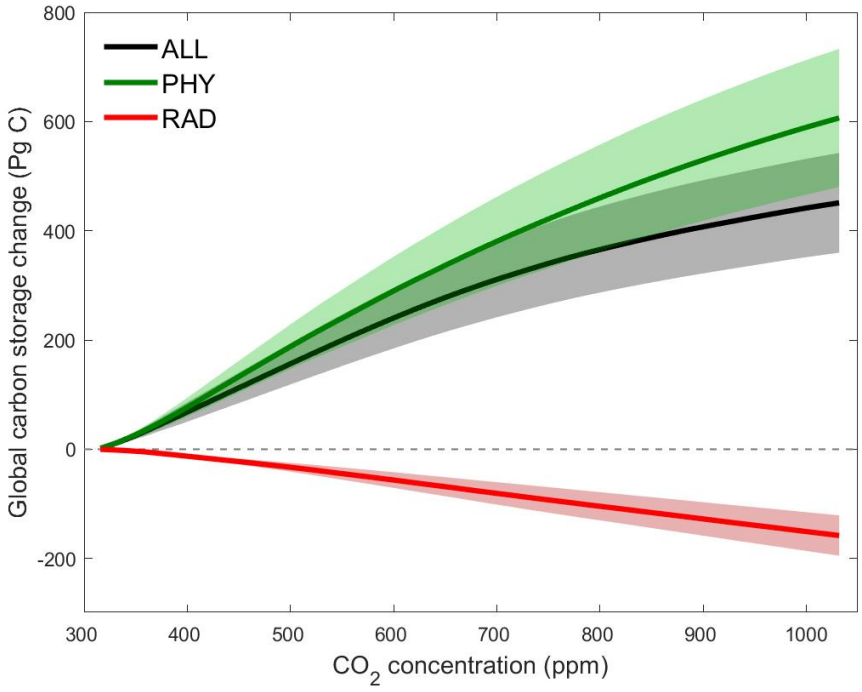

Supplementary Figure 2 The effects of land cover change on PHY-induced temperature and carbon storage change. a. Comparisons of temperature change induced by direct CO_2 physiological forcing (PHY_{dir}) for neighbouring pixels with and without land cover change across global vegetated land. Values shown for the HadGEM2-ES and MPI-ESM-LR, which both model land cover change. **b.** Comparisons of carbon storage change induced by PHY_{dir} for neighbouring pixels with and without land cover change, again for the HadGEM2-ES and MPI-ESM-LR models and for vegetated land. For comparison, the one-to-one line is marked as a thin grey dashed line.

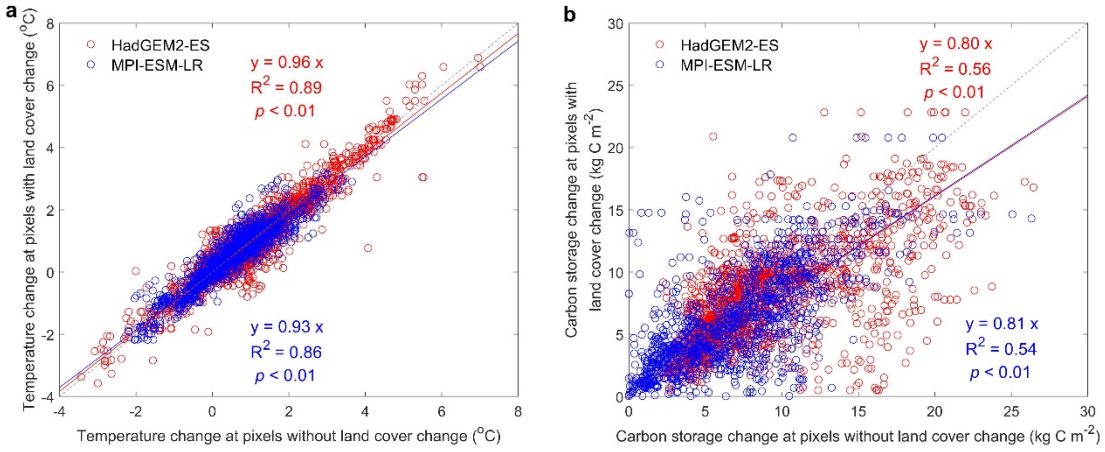

Supplementary Figure 3 Comparison of temperature change induced by vegetation physiological response to increased atmospheric CO_2 for all six ESMs analysed, and the subset of four ESM ensemble with fixed land cover. The total (PHY_{all}) and direct (PHY_{dir}) effect of CO_2 physiological forcing on temperature change are shown at quadrupled atmospheric CO_2. The four ESMs with fixed land cover are bcc-csm1-1, CanESM2, CESM1-BGC and IPSL-CM5A-LR, while the six-member ESM ensemble additionally includes HadGEM2-ES and MPI-ESM-LR. Each point represents a different location. For comparison, the one-to-one line is marked as a thin grey dashed line.

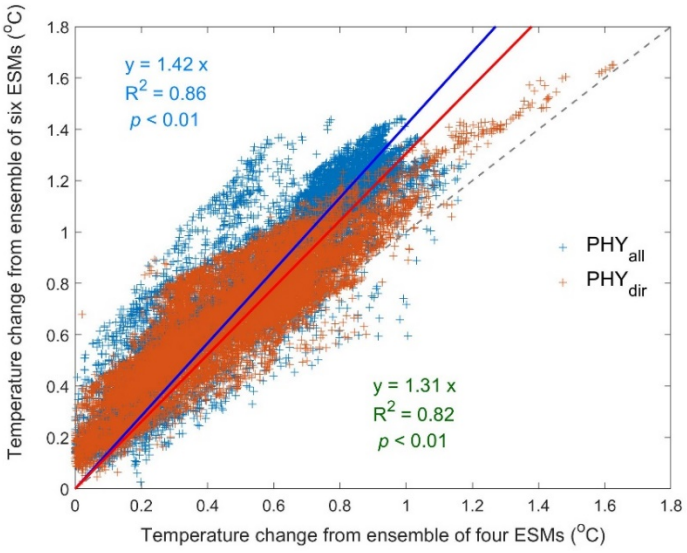

Supplementary Figure 4 Global patterns of temperature change induced by CO_2 physiological forcing from four and six ESMs at 4 × CO_2. Spatial distributions of temperature change through the total effect of CO_2 physiological forcing (PHY_{all}) from the predictions by a four (**a**) and six (**b**) ESM ensemble. The smaller ensemble (a subset of the six-member ensemble) all have fixed land cover. The temperature change is induced by the direct effect of CO_2 physiological forcing (PHY_{dir}) and responding to a 4 × CO_2 increase. The four ESMs include bcc-csm1-1, CanESM2, CESM1-BGC and IPSL-CM5A-LR, while six ESMs are bcc-csm1-1, CanESM2, CESM1-BGC, IPSL-CM5A-LR, HadGEM2-ES and MPI-ESM-LR.

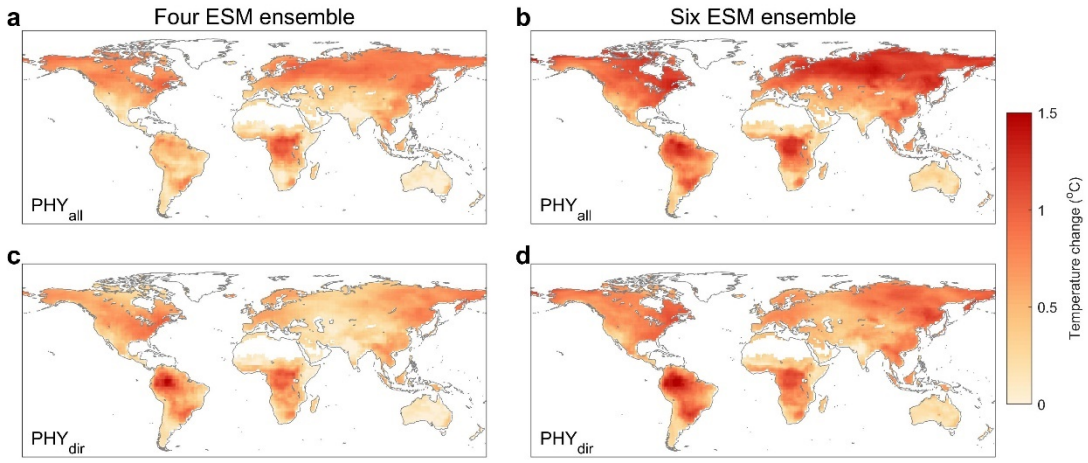

Supplementary Figure 5 Climate mitigation potential of terrestrial ecosystems. Global mean land air temperature change due to the total CO_2 physiological forcing (PHY_{all}), increased terrestrial carbon storage (BGC) and CO_2 radiative forcing (RAD) at 500 ppm (**a**), 800 ppm (**b**) and 4 × CO_2 (**c**). Shown are projections of three- and five-member ESM ensemble. The three-member ESMs are CanESM2, CESM1-BGC and IPSL-CM5A-LR, while five ESMs are CanESM2, CESM1-BGC, IPSL-CM5A-LR, HadGEM2-ES and MPI-ESM-LR, the extra two models having land cover changes. The bcc-cms1-1 model used elsewhere does not provide carbon storage data and so it is excluded for analysis here. The error bars represent the standard error of the models.

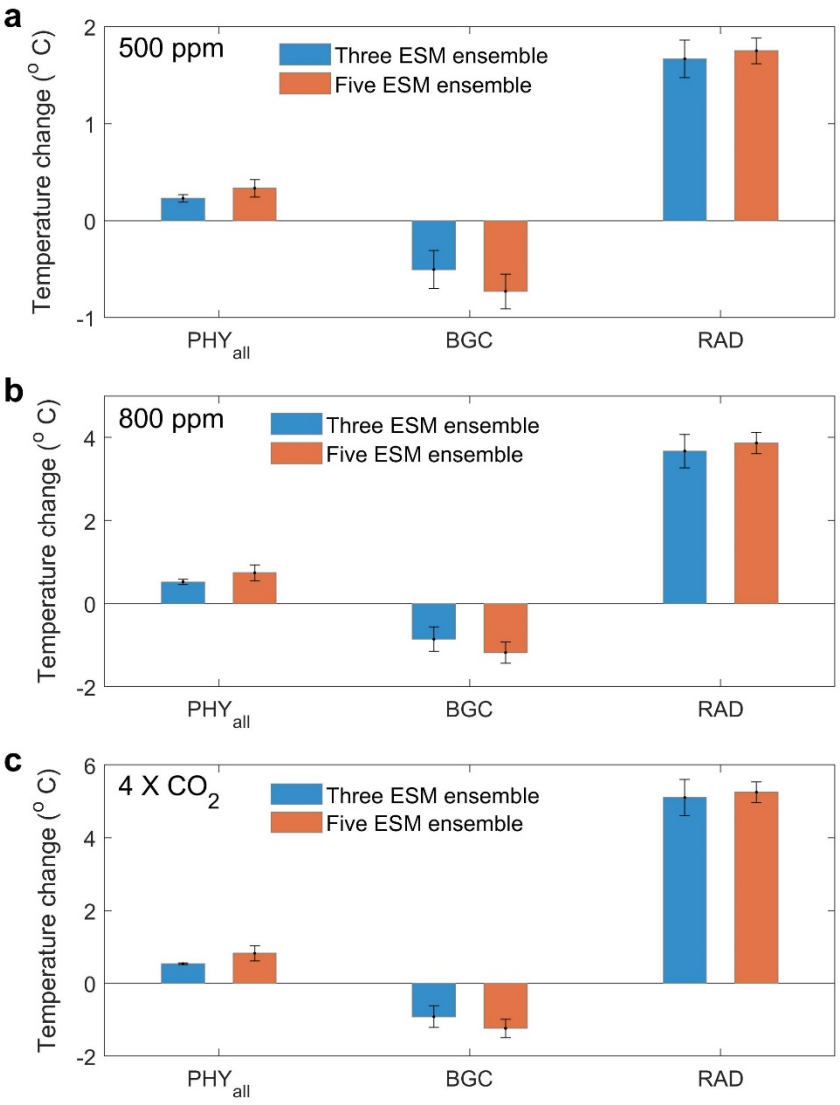
a
500 ppm
Three ESM ensemble
Five ESM ensemble
Temperature change (°C)
2
1
0
-1
PHY all
BGC
RAD
b
800 ppm
Three ESM ensemble
Five ESM ensemble
Temperature change (°C)
4
2
0
-2
PHY all
BGC
RAD
c
4 X CO2
Three ESM ensemble
Five ESM ensemble
Temperature change (°C)
6
4
2
0
-2
PHY all
BGC
RAD

76

Supplementary Figure 6 Climate forcing triggered by direct CO_2 physiological forcing in response to increasing atmospheric CO_2. a. Direct CO_2 physiological forcing (PHY_{dir}) with increasing atmospheric CO_2 triggers climate forcing associated with changes in albedo (α), aerodynamic resistance (r_a), evapotranspiration (ET), downwelling shortwave radiation (SW) and near surface air emissivity (ε_a). The changes in these variables are calculated using average data of every 20 years of the simulations. The resulting climate forcings values under 4 × CO_2 are plotted on the right side. The shaded areas represent the standard error of the selected models. **b.** Comparisons of five forcings induced by PHY_{all} and PHY_{dir} for a quadrupled CO_2 concentration. Results of the final 20 years are used. The error bars represent the standard error of each forcing.

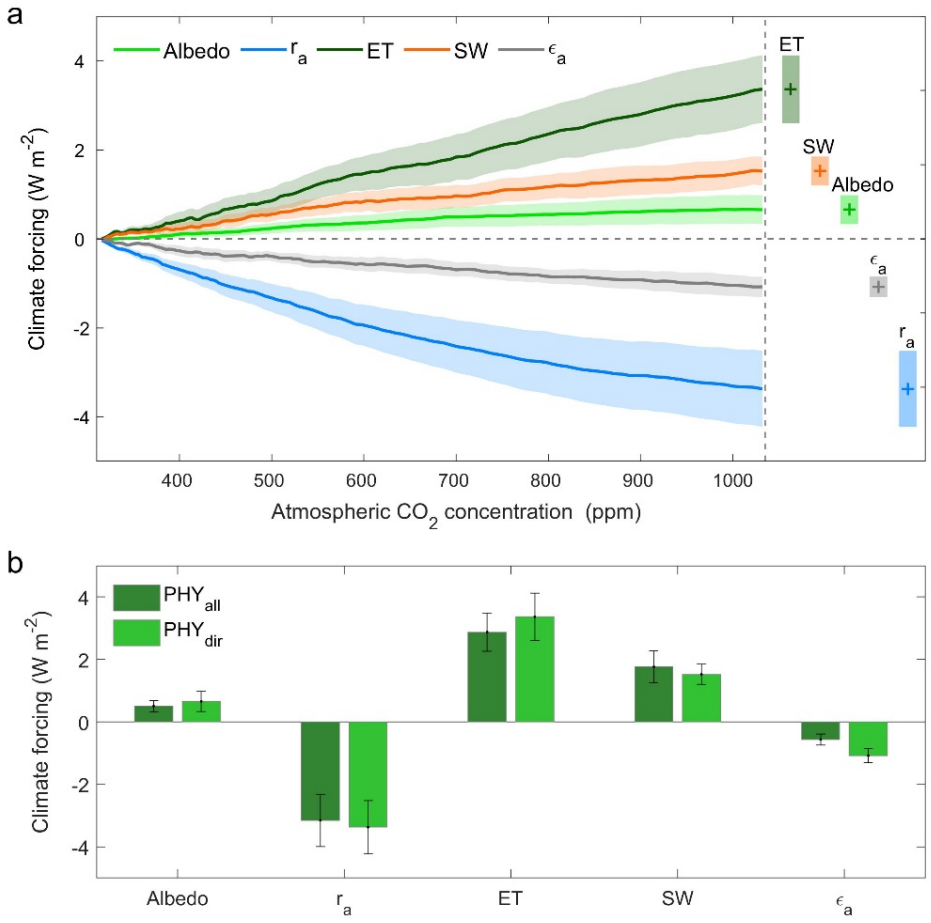
a
Albedo
r_a
ET
SW
ϵ_a
Climate forcing (W m^{-2})
Atmospheric CO_2 concentration (ppm)
b
PHY_{all}
PHY_{dir}
Climate forcing (W m^{-2})
Albedo
r_a
ET
SW
ϵ_a

88

Supplementary Figure 7 Change in global mean annual land air temperature and individual climate forcing components induced by vegetation physiological response to increasing atmospheric CO_2 for CMIP6 data. **a**. Global annual area-weighted temperature change of vegetated land induced by total CO_2 physiological forcing (PHY_{all}) and the direct CO_2 physiological forcing (PHY_{dir}) in response to increasing atmospheric CO_2 concentration. Shaded areas show the standard errors of the five Earth System Models (ESMs) used from CMIP6, including ACCESS-ESM1-5, BCC-CSM2-MR, CanESM5, IPSL-CM6A-LR and MPI-ESM1-2-LR, and the thick curves are their multi-model means. **b**. PHY_{all}-induced climate forcing associated with changes in albedo, aerodynamic resistance (r_a), evapotranspiration (ET), downwelling shortwave radiation (SW) and near-surface air emissivity (ε_a). The changes in these variables are calculated using a moving average with a 20-year window. The resulting values under $4 \times CO_2$ are plotted on the righthand side, with the "+" markers indicating multi-model means.

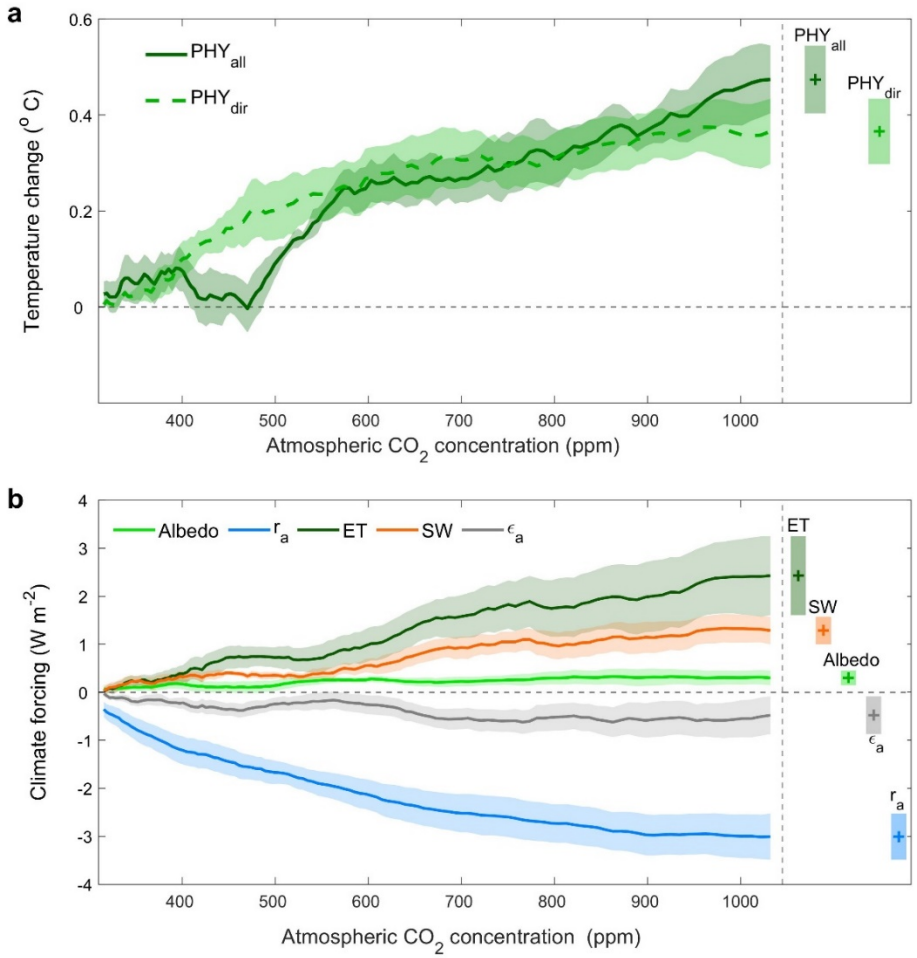
a
Temperature change (°C)
PHY_all
PHY_dir
Atmospheric CO2 concentration (ppm)
b
Climate forcing (W m-2)
Albedo
ra
ET
SW
εa
Atmospheric CO2 concentration (ppm)

103

Supplementary Figure 8 Comparisons of leaf area index (LAI) and transpiration changes driven by CO_2 physiological forcing and free-air CO_2 enrichment (FACE) measurements. a. Comparison of LAI changes due to elevated CO_2 at eight FACE sites (Obs) with those from the total CO_2 physiological forcing from multi-model means of six Earth system models (Model). **b.** Comparison of transpiration changes due to elevated CO_2 at eight FACE sites (Obs) and transpiration changes through the total CO_2 physiological forcing from multi-model means of six ESMs (Model). The ambient CO_2 is about 370 ppm and elevated CO_2 is about 570 ppm for most FACE sites. The ESM results are extracted for the same CO_2 ranges within each FACE site. The eight FACE sites include ASPEN (Uddling et al., 2009), BIOCON (Lee et al., 2001), DUKE (McCARTHY et al., 2007; Schäfer et al., 2002), EUC (Duursma et al., 2016), EURO (Liberloo et al., 2005), NEVADA (Newingham et al., 2013), OAK (Norby et al., 2003; Warren et al., 2011) and WEB (Bader et al., 2013). The error bars represent the standard deviations of six models.

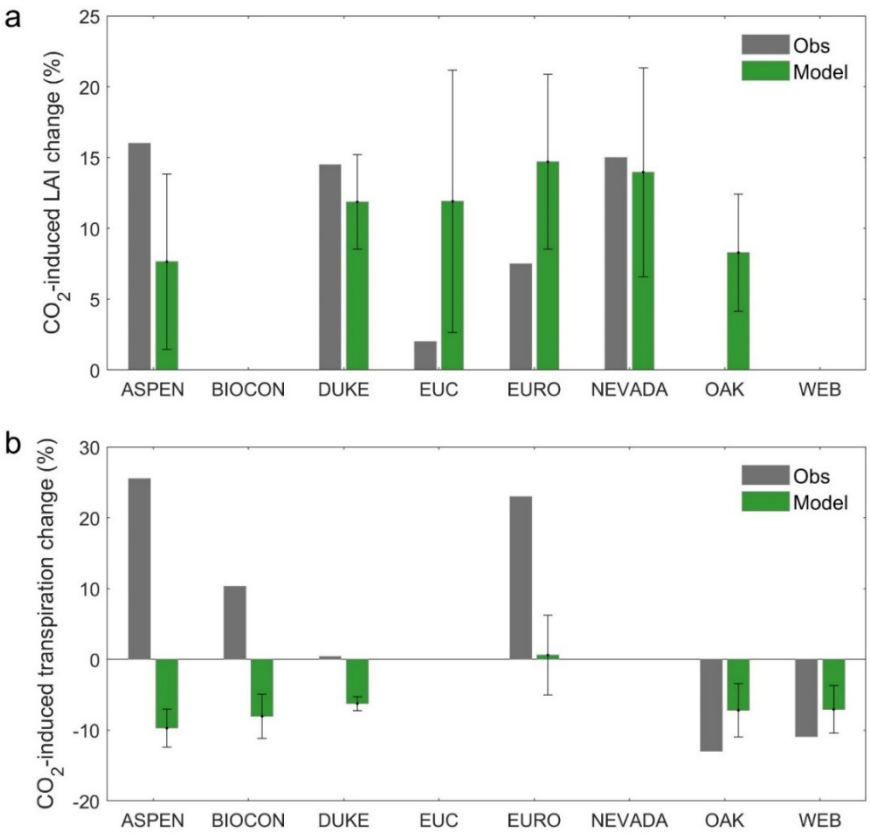
a
CO_2-induced LAI change (%)
25
20
15
10
5
0
Obs
Model
ASPEN
BIOCON
DUKE
EUC
EURO
NEVADA
OAK
WEB
b
CO_2-induced transpiration change (%)
30
20
10
0
-10
-20
Obs
Model
ASPEN
BIOCON
DUKE
EUC
EURO
NEVADA
OAK
WEB

118

Supplementary Figure 9 CO_2 physiological forcing induced changes in vegetation property and energy fluxes with increasing atmospheric CO_2. Changes in leaf area index (LAI) (**a, b**), cloud fraction (**c, d**) and net longwave radiation (**e, f**) through the total (PHY_{all}) and direct (PHY_{dir}) vegetation physiological response to rising atmospheric CO_2, respectively. PHY_{all} induced changes (**a, c, d**) are calculated as the difference between simulations of 1pctCO2 and esmFdbk1 for each model and multi-model ensemble. PHY_{dir} induced changes (**b, d, f**) are estimated as the difference between the simulations of each year and the average of the first 20 years in esmFixClim1. Both results are smoothed using a twenty-year running window, and area-weighted to obtain global average.

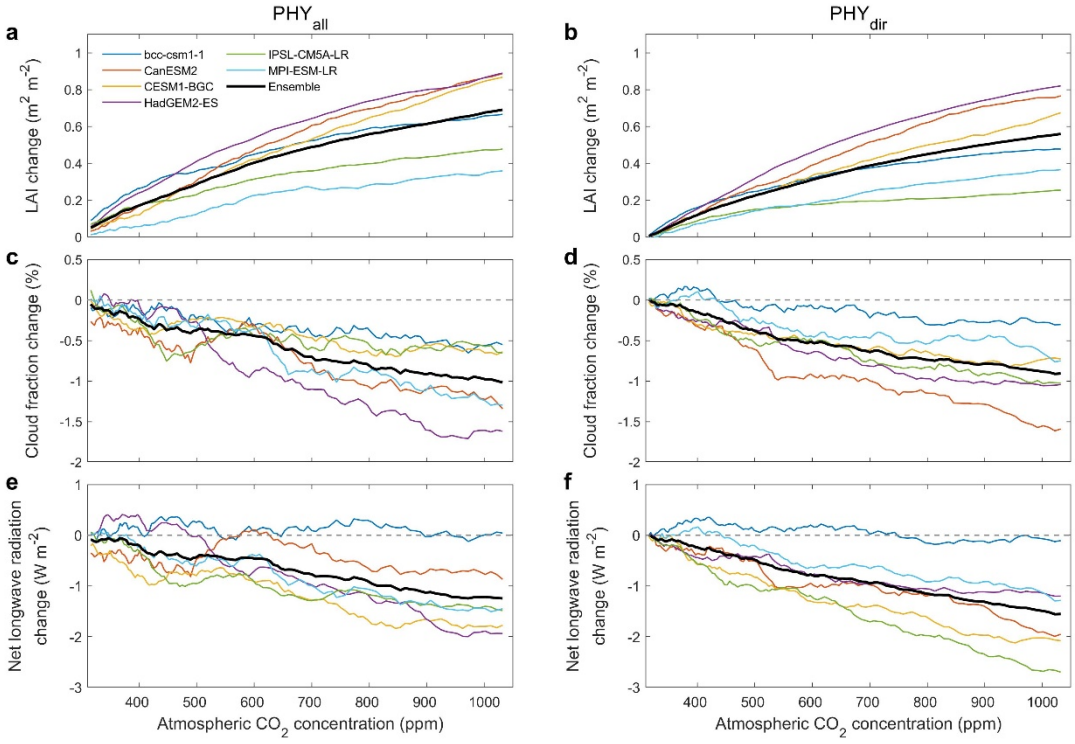

Supplementary Figure 10 Changes in vegetation biophysical factors induced by CO_2 physiological forcing with increasing atmospheric CO_2. CO_2 physiological forcing (PHY), including its total (PHY_{all}) and direct (PHY_{dir}) terms, induced changes in albedo (**a, b**), aerodynamic resistance (r_a) (**c, d**), evapotranspiration (ET) (**e, f**), downwelling shortwave radiation (SW) (**g, h**), near surface air emissivity (ε_a) (**i, j**), respectively. The changes of variables in each atmospheric CO_2 for the total PHY (PHY_{all}) are calculated as the difference between the simulations of 1pctCO2 and esmFdbk1 for each model and multi-model ensemble. Whereas, the changes of each variable for the direct PHY feedback (PHY_{dir}) are calculated as the difference between the simulations of each atmospheric CO_2 concentration and the average of the first 20 years in esmFixClim1. The results are smoothed using a twenty-year running window and area-weighted globally.

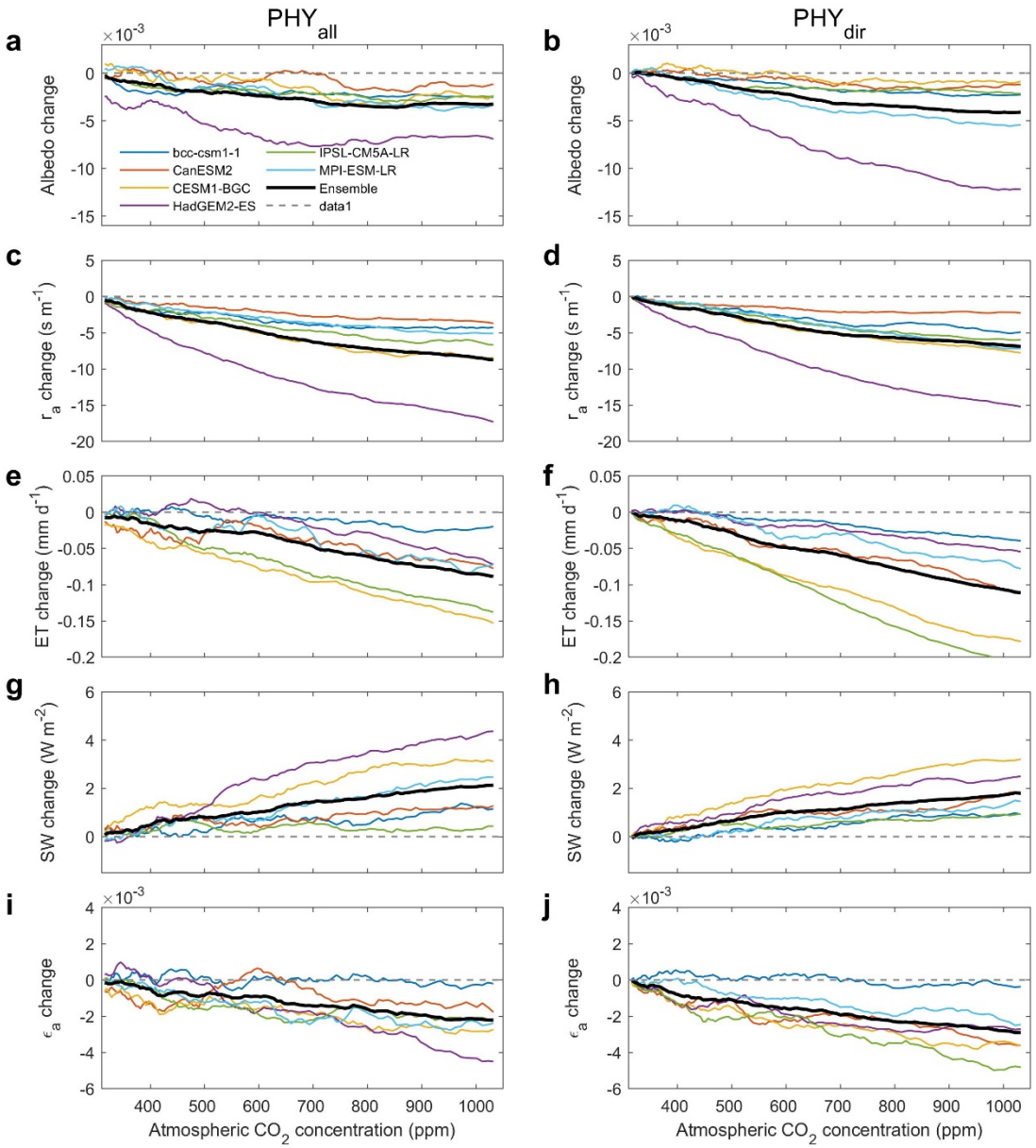
PHY all
PHY dir
a
b
c
d
e
f
g
h
i
j
Albedo change
r_a change (s m^{-1})
ET change (mm d^{-1})
SW change (W m^{-2})
ϵ_a change
×10^{-3}
bcc-csm1-1
CanESM2
CESM1-BGC
HadGEM2-ES
IPSL-CM5A-LR
MPI-ESM-LR
Ensemble
data1
Atmospheric CO$_2$ concentration (ppm)

142

Supplementary Figure 11 Regional contributions to temperature change by PHY and BGC under 500 ppm. a. Contribution of regional vegetation physiological responses (PHY_{all}; green bars) and increased carbon storage (BGC; blue bars) to the overall global temperature change for each of the IPCC AR5 SREX regions for 500 ppm. Bars represent area-weighted multi-model means, and the error bars indicate the standard errors of the models for each region. **b**. Spatial distributions of the net effects of warming induced by PHY_{all} and cooling through BGC for atmospheric CO_2 level of 500 ppm.

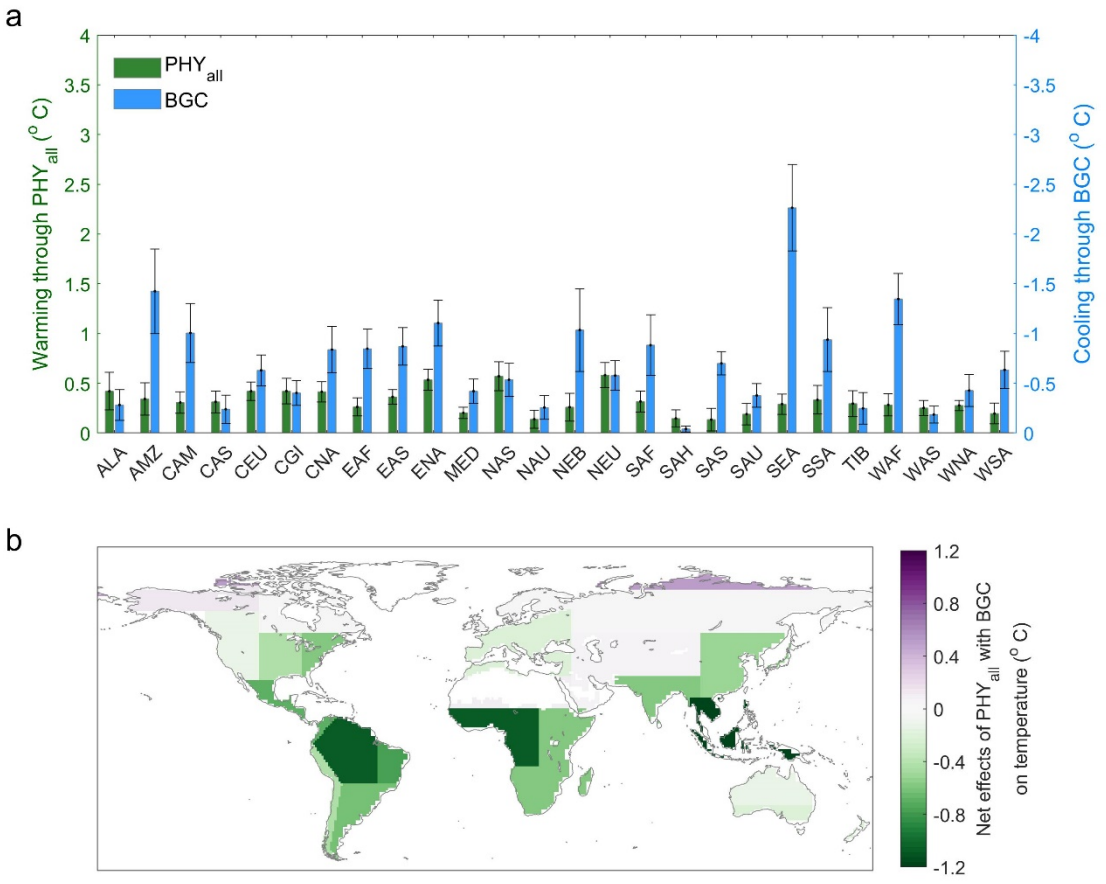

Supplementary Figure 12 Spatial patterns of CO_2 physiological forcing relative to radiative forcing on temperature change in response to 4 × CO_2. **a**. Spatial patterns of the ratio of total CO_2 physiological forcing (PHY_{all}) induced temperature change relative to that of CO_2 radiative forcing (RAD) from multi-model ensemble over global vegetated lands in response to a quadrupling of CO_2. **b**. Variations of the ratio of direct CO_2 physiological forcing (PHY_{dir}) induced temperature change relative to that of RAD over global vegetated lands under 4 × CO_2. The data from the final 20 years of PHY_{all}, PHY_{dir} and RAD induced temperature is used here.

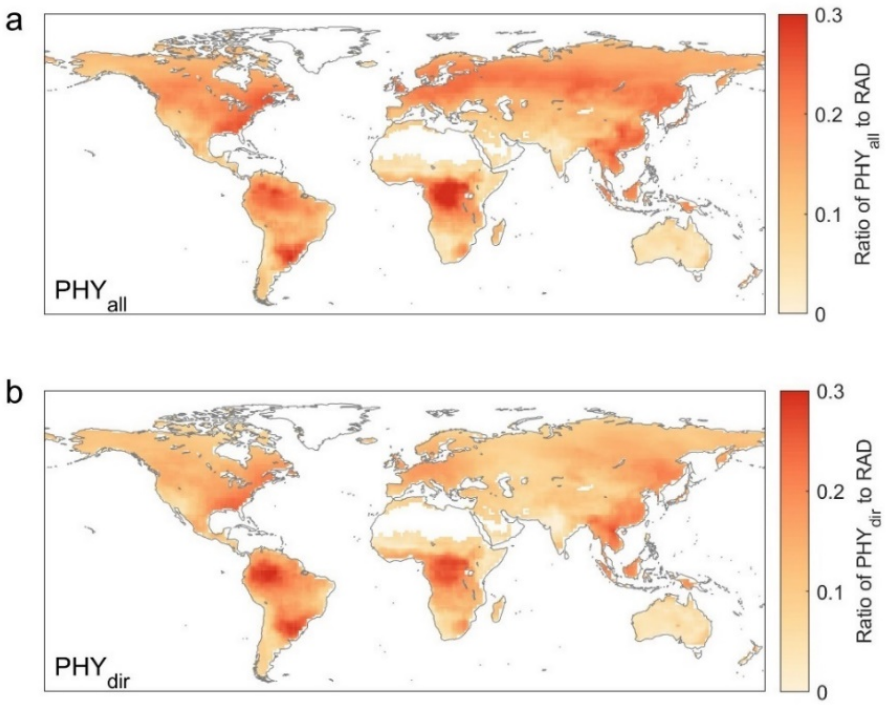

Supplementary Figure 13 Global patterns of temperature change and climate forcing through vegetation physiological response to 4 × CO_2. Spatial distributions of temperature change induced by **a.** total CO_2 physiological forcing (PHY_{all}) and **b.** interactive terms (PHY_{int}) in response to 4 × CO_2. The spatial patterns of climate forcings by PHY_{all} and PHY_{int} associated with changes in **c-d.** albedo (α), **e-f**. aerodynamic resistance (r_a), **g-h**. evapotranspiration (ET), **i-j**. downwelling shortwave radiation (SW) and **k-l**. near surface air emissivity (ε_a) using estimations of the final 20 years (~ 1032 ppm) are shown, respectively.

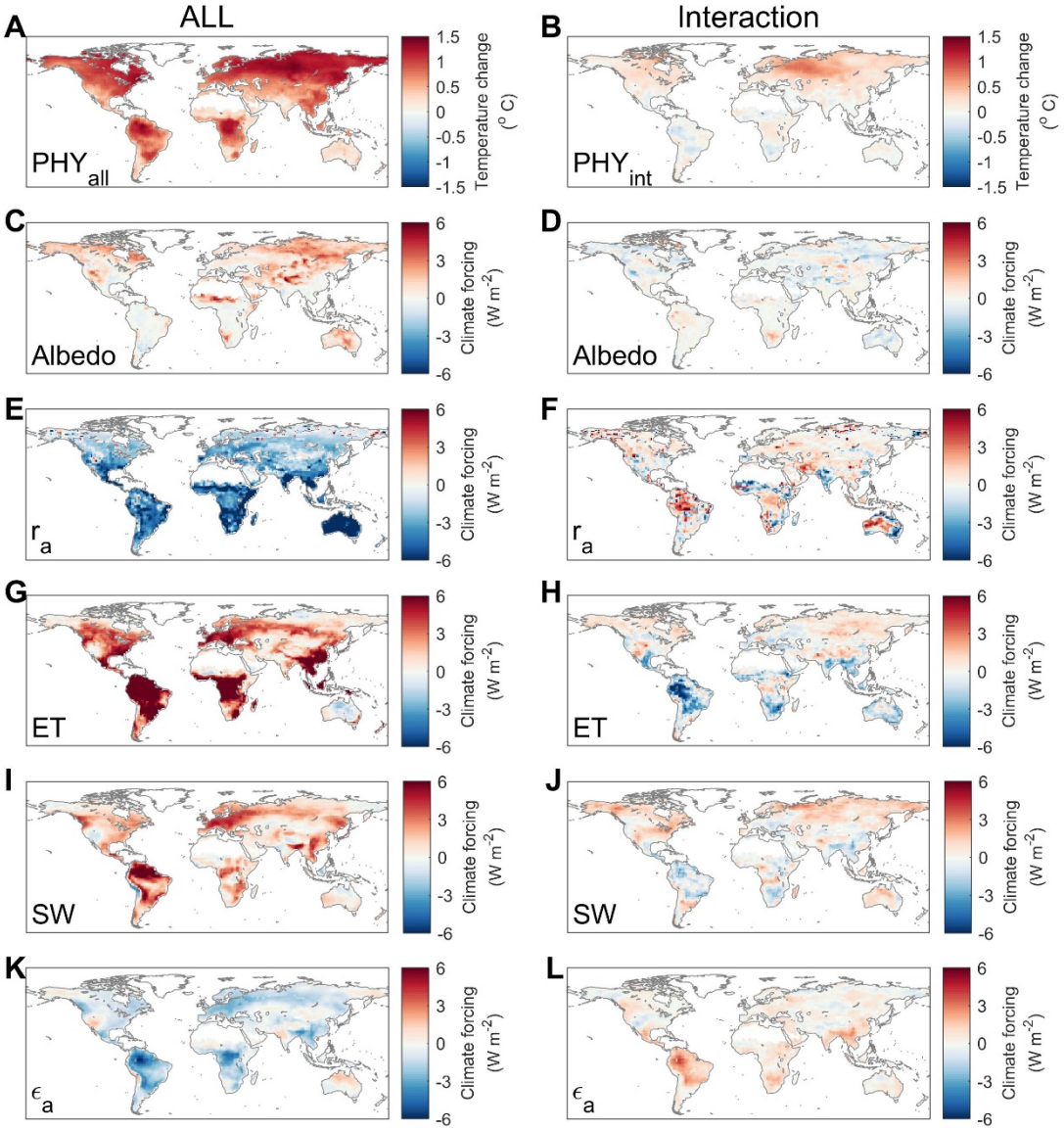
A
ALL
B
Interaction
PHY all
PHY int
C
D
Albedo
E
F
r a
G
H
ET
I
J
SW
K
L
ϵ a
1.5
1
0.5
0
-0.5
-1
-1.5
Temperature change (° C)
6
3
0
-3
-6
Climate forcing (W m-2)

168

Supplementary Figure 14 Global patterns of model agreement for 4 × CO_2. Spatial distributions of model agreement across six ESMs over global vegetated land for **a.** total (PHY_{all}), **b.** direct (PHY_{dir}) and **c.** interactive (PHY_{int}) effects of vegetation physiological responses on local warming under 4 × CO_2. The data of the final 20 years is used

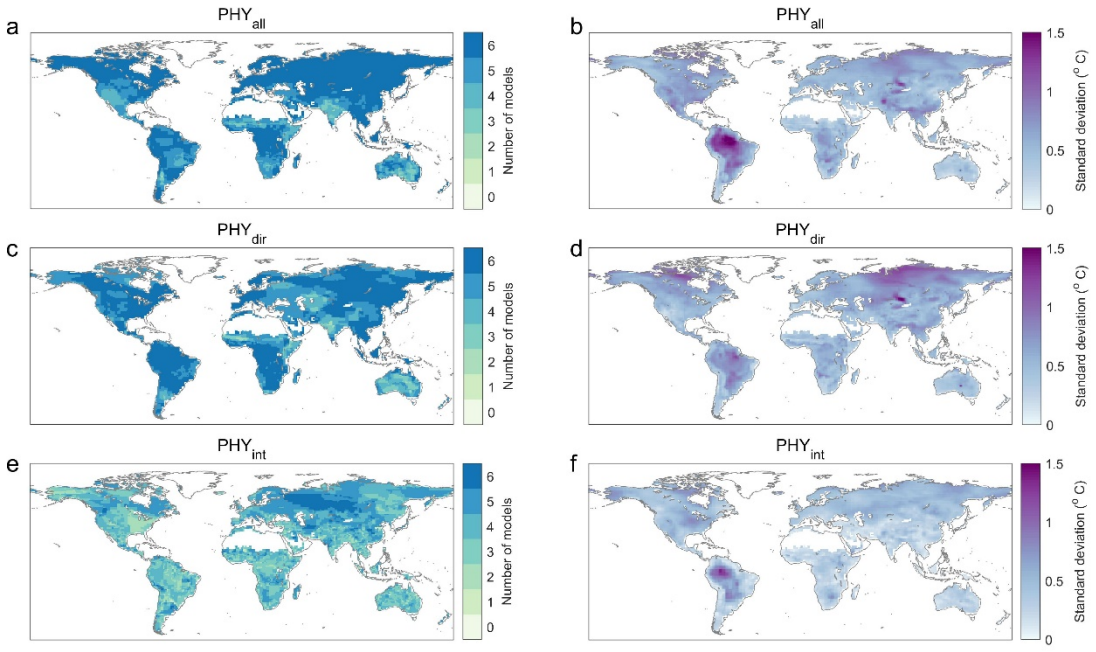

Supplementary Figure 15 Spatial pattern of CO_2 physiological forcing induced vegetation biophysical factor and cloud fraction changes. Leaf area index (LAI) changes (**a, b**), evapotranspiration (ET) changes (**c, d**) and cloud fraction changes (**e, f**) through total (PHY_{all}) and direct (PHY_{dir}) vegetation physiological response to 4 × CO_2, respectively. The results from the multi-model ensemble over the final 20 years are shown.

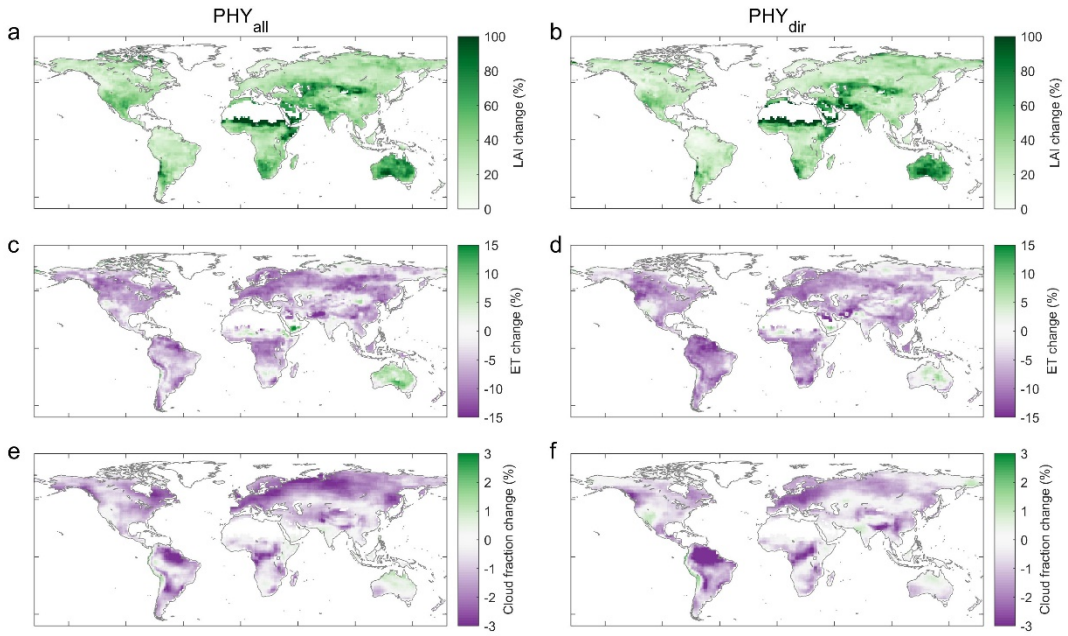

Supplementary Figure 16 Global patterns of temperature change and climate forcing through vegetation physiological in response to CO_2 concentration of 500 ppm. **a.** Spatial distributions of temperature change induced by direct CO_2 physiological forcing (PHY_{dir}) under 500 ppm. The spatial patterns of climate forcings by PHY_{dir} associated with changes in **b.** albedo, **c**. aerodynamic resistance (r_a), **d**. evapotranspiration (ET), **e**. downwelling shortwave radiation (SW) and **f**. near surface air emissivity (ε_a) under atmospheric CO_2 concentration of 500 ppm are shown, respectively.

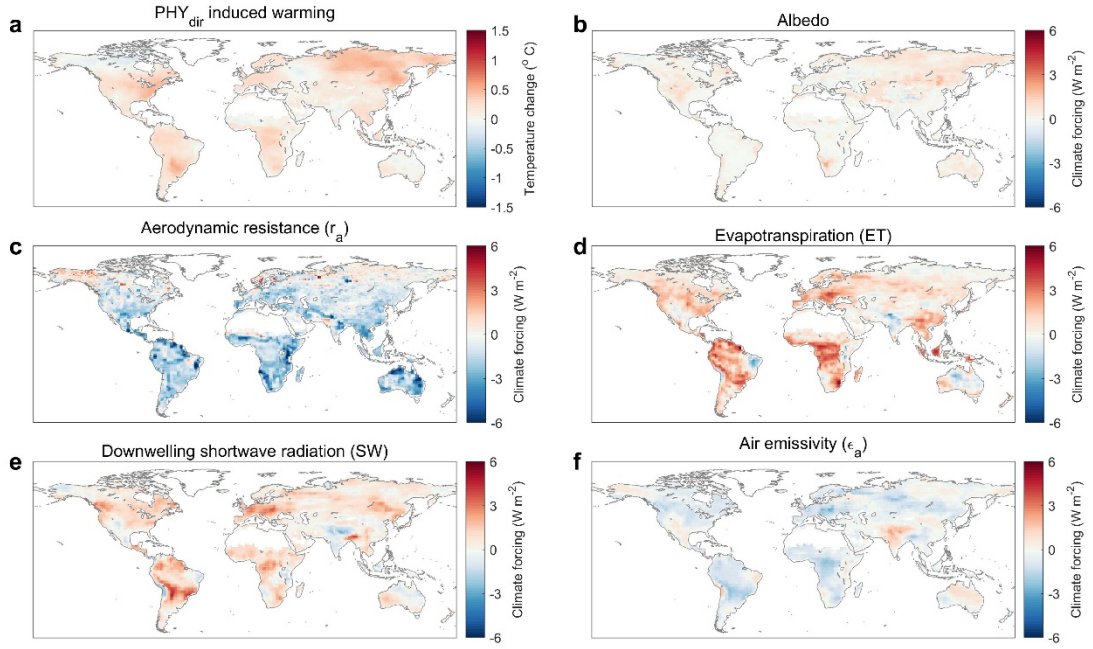

Supplementary Figure 17 Vegetation biophysical properties changes by CO_2 physiological forcing in response to 4 × CO_2. **a.** variations of percentage of leaf area index (LAI) change induced by total (PHY_{all}) and direct (PHY_{dir}) CO_2 physiological forcing with baseline LAI gradients in response to quadrupled CO_2. **b.** changes in PHY_{all} and PHY_{dir} induced evapotranspiration (ET) with baseline LAI gradients under 4 × CO_2. PHY_{all}- and PHY_{dir}-induced LAI and ET changes are binned with every 0.1 baseline LAI varying from 0 to 6, and the percentage of LAI changes relative to baseline LAI is estimated. The shaded areas indicate the standard error among different models. The binned LAI and ET changes along baseline LAI gradients are smoothed using a five-bin running window.

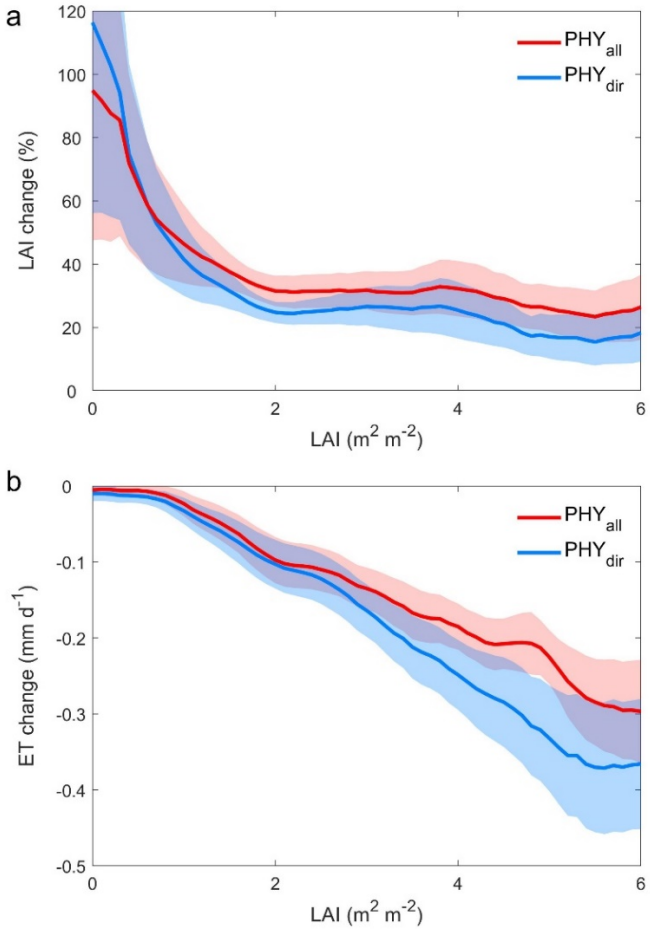

Supplementary Figure 18 Global patterns of temperature, leaf area index (LAI) and evapotranspiration (ET) changes from our results and the last 20 years of RCP8.5. Spatial distributions of temperature (**a-c**), LAI (**d-f**) and ET (**g-i**) changes induced by the coupled simulations (ALL) of cumulative 1% per year increase in atmospheric CO_2 at 4 × CO_2 in **a, d, g,** at 800 ppm in **b, e, g,** and ESM simulations of the last 20 years under the RCP8.5 scenario in **c, f, i**.